Evaluation of spatial-temporal dynamics in surface water temperature of Qinghai Lake from 2001 to 2010 by using MODIS data

ARTICLE *in* JOURNAL OF ARID LAND · DECEMBER 2013

Impact Factor: 0.79 · DOI: 10.1007/s40333-013-0188-5

6 AUTHORS, INCLUDING:

Fei Xiao

22 PUBLICATIONS **199** CITATIONS

SEE PROFILE

Feng Ling

Chinese Academy of Sciences

40 PUBLICATIONS **312** CITATIONS

SEE PROFILE

Yun Du

Nanjing University

36 PUBLICATIONS **197** CITATIONS

SEE PROFILE

Qi Feng

Chinese Academy of Sciences

12 PUBLICATIONS **37** CITATIONS

SEE PROFILE

J Arid Land (2013) 5(4): 452–464
doi: 10.1007/s40333-013-0188-5
jal.xjegi.com; www.springer.com/40333

Evaluation of spatial-temporal dynamics in surface water temperature of Qinghai Lake from 2001 to 2010 by using MODIS data

Fei XIAO*, Feng LING, Yun DU, Qi FENG, Yi YAN, Hui CHEN

Institute of Geodesy and Geophysics, Chinese Academy of Sciences, Wuhan 430077, China

Abstract: Lake surface water temperature (SWT) is an important indicator of lake state relative to its water chemistry and aquatic ecosystem, in addition to being an important regional climate indicator. However, few literatures involving spatial-temporal changes of lake SWT in the Qinghai-Tibet Plateau, including Qinghai Lake, are available. Our objective is to study the spatial-temporal changes in SWT of Qinghai Lake from 2001 to 2010, using Moderate-resolution Imaging Spectroradiometer (MODIS) data. Based on each pixel, we calculated the temporal SWT variations and long-term trends, compared the spatial patterns of annual average SWT in different years, and mapped and analyzed the seasonal cycles of the spatial patterns of SWT. The results revealed that the differences between the average daily SWT and air temperature during the temperature decreasing phase were relatively larger than those during the temperature increasing phase. The increasing rate of the annual average SWT during the study period was about 0.01°C/a, followed by an increasing rate of about 0.05°C/a in annual average air temperature. The annual average SWT from 2001 to 2010 showed similar spatial patterns, while the SWT spatial changes from January to December demonstrated an interesting seasonal reversion pattern. The high-temperature area transformed stepwise from the south to the north regions and then back to the south region from January to December, whereas the low-temperature area demonstrated a reversed annual cyclical trace. The spatial-temporal patterns of SWTs were shaped by the topography of the lake basin and the distribution of drainages.

Keywords: surface water temperature (SWT); spatial-temporal changes; MODIS; Qinghai Lake

Citation: Fei XIAO, Feng LING, Yun DU, Qi FENG, Yi YAN, Hui CHEN. 2013. Evaluation of spatial-temporal dynamics in surface water temperature of Qinghai Lake from 2001 to 2010 by using MODIS data. Journal of Arid Land, 5(4): 452–464. doi: 10.1007/s40333-013-0188-5

Lake surface water temperature (SWT) indicates the temperature of an extremely thin layer in the lake surface (Becker and Daw, 2005). It is an important indicator of lake state and exerts a strong influence on water chemistry and aquatic ecosystem (Arnell et al., 1996; Trumpickas et al., 2009). At the same time, lake SWT has a driving effect on the regional weather and climate in the surrounding areas of large lakes (Livingstone, 2003). Therefore, lake SWT is also an energy balance indicator in studying the interactions and energy fluxes between the atmosphere and the lake (Alcântara et al., 2010). Traditionally, lake SWT data are collected from *in situ* measurements. However, *in situ* measurement data are often spatially sparse, and very few *in situ* measurements are available at suitable locations and time (Trumpickas et al., 2009). Additionally, *in situ* measurements are expensive and time consuming (Alcântara et al., 2010). Water temperature data with better spatial and temporal resolutions are needed in many applications, such as climate change monitoring, studies on hydrological cycle, aquatic organism habitat, fishery and aquaculture, and water-quality management (Ekercin and Örmeci, 2010; Rani et al., 2011).

*Corresponding author: Fei XIAO (E-mail: xiaof@whigg.ac.cn)
Received 2012-10-31; revised 2013-01-26; accepted 2013-03-07

In recent decades, satellite observations have provided an attractive method of monitoring SWT at fine spatial and temporal scales. However, most studies concentrated on sea SWT. Well-established practices of sea SWT monitoring have been widely carried out in oceanography (Barton and Prata, 1995; Emery and Yu, 1997; Parkinson, 2003). Recently, space-based thermal data have been increasingly used to monitor the surface temperature of inland water bodies, including lakes (Bussières and Schertzer, 2004; Plattner et al., 2006; Reinart and Reinhold, 2008) and streams (Torgersen et al., 2001; Handcock et al., 2006; Hook et al., 2007). The data used in SWT monitoring range from microwave to thermal infrared images with different spatial, temporal, and radiometric resolutions, such as Scanning Multichannel Microwave Radiometer (SMMR) and Special Sensor Microwave/Imager (SSM/I) (Fily et al., 2003), Advanced Very High Resolution Radiometer (AVHRR) (Wooster et al., 2001; Chavula et al., 2009), Along Track Scanning Radiometer (ATSR) (Schneider et al., 2009), Landsat (Wloczyk et al., 2006), Moderate-resolution Imaging Spectroradiometer (MODIS) (Reinart and Reinhold, 2008), and infrared videography (Li et al., 2000). Due to their high temporal resolution, large spectral range, and high radiometric sensitivity, MODIS products have attracted increasing interests in lake temperature studies in recent years. Many studies showed that the MODIS thermal bands can successfully measure inland SWT with considerable accuracy (Hook et al., 2007; Reinart and Reinhold, 2008; Schneider et al., 2009; Alcântara et al., 2010).

Qinghai-Tibet Plateau has been suggested to be susceptible to future climate change (Sha et al., 2002; Zheng et al., 2002; Zhao et al., 2004; Wu et al., 2005; Zhu and Chang, 2011). Qinghai Lake, located in the northeast of the Qinghai-Tibet Plateau, is the largest inland saltwater lake in China. Owing to its high altitude, closed catchment, and low-intensity human activities, Qinghai Lake is, to some extent, an ideal location to directly study the environmental effects of climate change. However, *in situ* observation data of Qinghai Lake are very scarce, and obtaining spatial variety of SWT changes in large surface areas using limited *in situ* data is also very difficult. To our knowledge, few literatures involving spatial-temporal changes of lake SWT in the Qinghai-Tibet Plateau, including Qinghai Lake, are available. The objectives of this paper are to study the seasonal and inter-annual fluctuations of SWT in Qinghai Lake, analyze its responses to climate change, and map the spatial pattern changes of SWT using MODIS time-series data from 2001 to 2010.

1 Study area

Qinghai Lake is an inland saltwater lake at 36°33'–37°14'N and 99°37'–100°45'E (Fig. 1). It is the largest saline lake in China with a closed catchment (Wang et al., 2011). The drainage area of Qinghai Lake is approximately 29,600 km^2, and the lake area is about 4,300 km^2. The water surface altitude is roughly 3,193.6 m, and the average depth of the lake is 21 m. At the aforementioned water level, the lake storage is approximately 73.8×10^9 m^3. Two small islands are located in the Qinghai Lake, namely, Haixinshan and Sankuaishi. The area of Haixinshan is approximately 1.0 km^2, whereas that of Sankuaishi is only 0.05 km^2. Located in a semi-arid zone of Northwest China, the average annual precipitation of Qinghai Lake is approximately 350 mm based on the recent 50-year record. Qinghai Lake is also an inland wetland included in the Ramsar Convention List of Wetlands of International Importance. In addition to its great importance in the conservation of biodiversity and hydro-ecological functions, Qinghai Lake is very sensitive to global changes. Since the beginning of record keeping in 1959, the water level of Qinghai Lake has dropped by over 3.4 m, whereas the salinity has increased by 2.05 g/L (Liu et al., 2009).

2 Materials

In this study, MODIS thermal-infrared imagery on board the Earth Observing System Terra platform was employed to analyze the spatial and temporal variations of SWT in Qinghai Lake. According to classification-based emissivity estimation, thermal-infrared bands 31 and 32 (11.0–12.0 μm) were proven to have high emissivities and relatively stable average emissivities within 0.01 for many land cover types, including lake surfaces (Wan and Dozier, 1996;

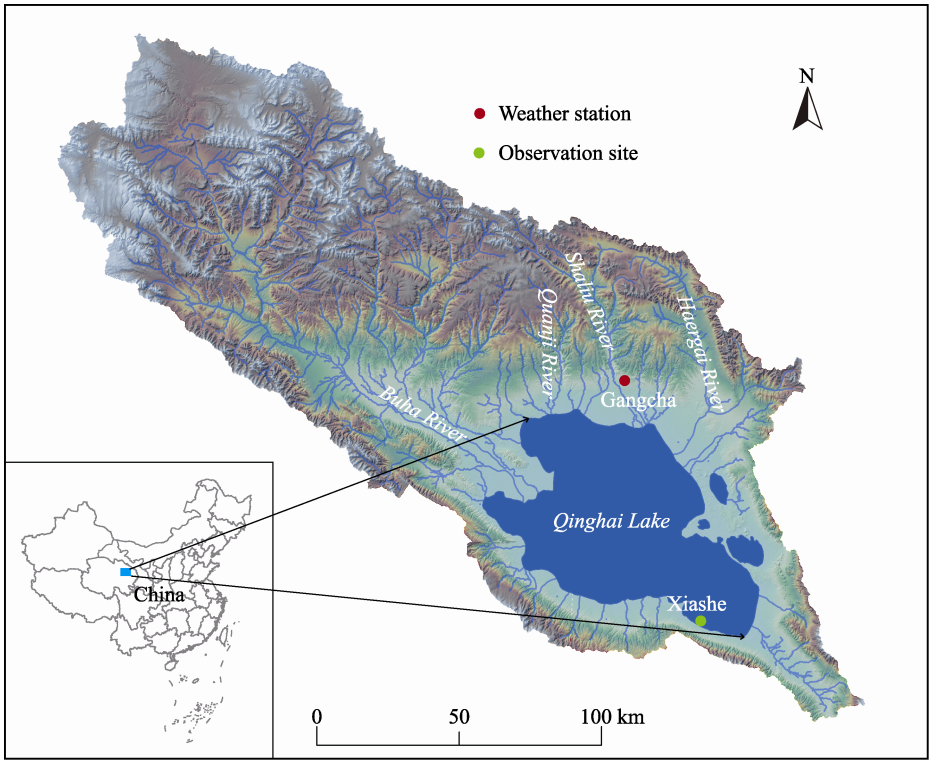

Fig. 1 Location of Qinghai Lake in China

Wan, 1999). These two thermal-infrared channels were used to generate MODIS Land Surface Temperature (LST) Level 2, a 1-km spatial resolution at nadir product (MOD11_L2), by employing a generalized split-window algorithm (Wan and Dozier, 1996). Based on MOD11_L2, a daily Level 3 LST product at nominal 1-km spatial resolution (MOD11A1) was constructed by gridding the MOD11_L2 LST swath files into a sinusoidal projection. We adopted the V5 MOD11A1 product in this paper. Under clear-sky conditions, the accuracy specification of MODIS LST is 1 K in most cases, and an absolute accuracy of 0.5 K for calm lake water can be achieved after calibration using accurate ground measurements (Wan et al., 2002, 2004; Wang, 2008). Many studies have validated the accuracy of MODIS LST products in different lakes. The absolute differences between the MODIS products and *in situ* temperatures in Lake Geneva and Lake Constance were observed to range from 0.8 to 1.9 K (Oesch et al., 2005), while the differences were approximately 0.41 K for Lakes Vänern and Vättern (Reinart and Reinhold, 2008) and less than 0.1 K for Lake Tahoe (Schneider et al., 2009). Crosman and Horel (2009) observed a cool bias of –1.5 K for MODIS-derived SWT in the Great Salt Lake.

In this paper, we validated the MODIS-derived SWT of Qinghai Lake using *in situ* SWT data obtained from the Hydrology and Water Resources Survey Bureau of Qinghai Province. The SWT observation site was located in the southeast of the lake and named Xiashe (Fig. 1). The *in situ* observation time was near the satellite passing time, approximately 10:30 a.m. local solar time.

Relationship between air temperature and water temperature has been noticed and some efforts have been made to predict the water temperature using air temperature data (Kothandaraman and Evans, 1972; Cho and Lee, 2012). In this paper, we compared the MODIS-derived SWT of Qinghai Lake with air temperature data observed by Gangcha weather station. Gangcha weather station is located to the north of Qinghai Lake, and is the nearest weather station with a distance of 10 km away from the lakeshore (Fig. 1). The elevation of the Gangcha weather station is 3,301.5 m, which is about 102 m higher than the water

surface of Qinghai Lake. Air temperature was observed four times during one day in the weather station, at 02:00 a.m., 08:00 a.m., 14:00 p.m., and 20:00 p.m., respectively. However, the released data were only the averaged values of the observations. There was desynchrony in the observation time between the MODIS data and the daily mean temperature obtained from the weather station.

3 Methods

In this paper, the V5 MOD11A1 LST product was obtained from the NASA Land Processes Distributed Active Archive Center. The time when MODIS passes over Qinghai Lake is approximately at 10:30 a.m. local solar time. All available MODIS Terra images from 2001 to 2010 were used. Subsequently, LST spatially adjacent images were mosaicked using MODIS Reprojection Tool, and the areas that cover the entire Qinghai Lake were extracted. In addition, daily daytime 1-km grid LST (LST_Day_1 km) and quality control for daytime LST (QC_Day) data sets of the V5 MOD11A1 LST product were remapped to the Albers equal-area projection and converted from the input HDF-EOS to GeoTIFF format. Afterwards, the water body area was extracted from the MOD11A1 LST images using the shoreline interpreted from Landsat ETM+ imagery captured on 9 September 2005. Considering water fluctuation and the consequent sub-pixel interference in LST, we eliminated LST imagery pixels within a 2-km buffer area of the shoreline. Considering the islet areas and their effects on SWT, we removed the Haixinshan buffer area during the data processing.

For the removal of cloud-contaminated pixels and other questionable pixels coming from sources other than clouds, such as emissivity error and poor input data, items that included mandatory quality assurance, data quality, cloud, and LST quality flags in the QC_Day scientific data sets were adopted to evaluate pixel availability of all LST images. Pixels that had an average emissivity error greater than 0.02 or an average LST error greater than 2 K were eliminated. Thereafter, the spatial and temporal variations of annual and inter-annual SWT changes in Qinghai Lake were analyzed. The data-quality evaluation processing and the subsequent data statistics were completed using algorithms developed in MATLAB software. The spatial-temporal analysis employed the advantage of the ArcGIS software.

The average daily SWT of the entire Qinghai Lake was then calculated from the MOD11A1 LST data. After elimination of the questionable pixels, large amounts of null-value pixels were found in the LST dataset. For some days from 2001 to 2010, no available pixel or very limited valuable pixels were found in the whole lake area. Data discontinuity has been a known problem that often affects the result of data statistics. In this paper, the daily SWT of Qinghai Lake was calculated by averaging all available pixels in the lake area first. With regard to days when usable pixels in the whole region were unavailable, the daily SWT were deduced by linear interpolation method using data before and after these days to fill the data gaps.

Air temperature has been identified as an important factor influencing water temperature as heat transformation between water and air occurs at their contact interface (Alcântara et al., 2010). Therefore, comparison of the air temperature time series and the SWT would indicate the Qinghai Lake SWT responses to fluctuation in air temperature during the MODIS passing time. Observation data from Gangcha weather station from 2001 to 2010 were used in this paper. The relationships between air temperature and SWT during different periods were analyzed. Subsequently, the monthly average SWT and air temperature were calculated. Then, the annual average SWT and air temperature were also calculated and compared.

Seasonal SWT cycles were indicated by the 10-year average daily temperature values. Then, the time with the coldest and warmest water was determined, and the average time of freeze-up and break-up dates of Qinghai Lake was investigated using the MOD11A1 LST data. Thereafter, SWT inter-annual variability and its long-term trends were tested and analyzed using the average SWT time series over each month and year. Linear regression method was applied to determine the SWT trends.

The SWT spatial differences were analyzed under

different time scales. Some data gaps existed in the SWT data time series for each pixel resulting from the elimination of questionable pixels during data processing and the pixels not produced in the LST data. In this paper, the missing data of each pixel were also replaced by interpolated values. Monthly and annual average SWTs were calculated based on each pixel in the entire lake area. The spatial patterns of average SWT of Qinghai Lake in different years were then compared. Thereafter, the seasonal cycles of SWT spatial patterns were mapped and analyzed.

4 Results and discussion

4.1 Differences between MODIS-derived SWT and *in situ* observations of SWT

The *in situ* daily SWT data were measured at the depth of 0.5 m below water surface in July 2010 and July 2011. Although the SWT data of 2011 is not in the period of this study, it was still used here considering the sparseness of validation data. After the removal of the days with no available MODIS-derived SWT data in the observation site, there were 35 days remained for the data validation. The MODIS-derived SWT data are plotted against *in situ* observed SWT in Fig. 2. The Root-Mean-Square Deviation (RMSD) between MODIS-derived SWT and *in situ* observations of SWT was 1.46°C. Linear relationship between MODIS-derived SWT and *in situ* measured SWT can be observed from the figure, and the adjusted R-square was 0.526. Bias between the satellite observations and *in situ* data was about 0.19°C during the observation period. Although the sparseness of validation data and the differences in the observation depth and range between the satellite and *in situ* measurement may bring some deviations to the data validation, the MODIS-derived SWT still showed its applicability in estimating the thermodynamical features of the lake.

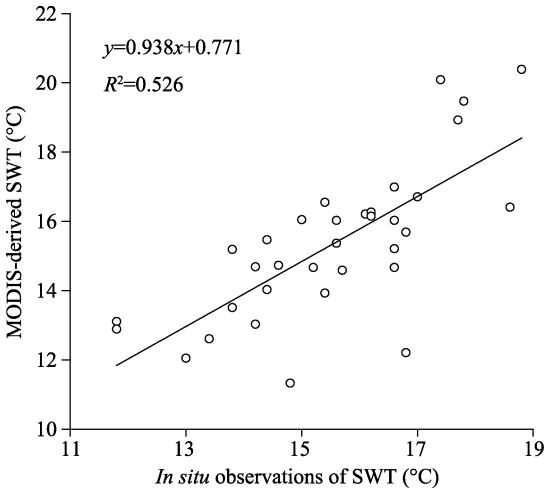

Fig. 2 Scatter plots of MODIS-derived surface water temperature (SWT) versus *in situ* observations of SWT in July 2010 and July 2011

4.2 Temporal changes in SWT

The daily SWT and the daily air temperature of Qinghai Lake during satellite passing time from 2001 to 2010 are shown in Fig. 3. In general, the daily variations of SWT and air temperature coincided with each other, although the SWT was higher than the air tem-

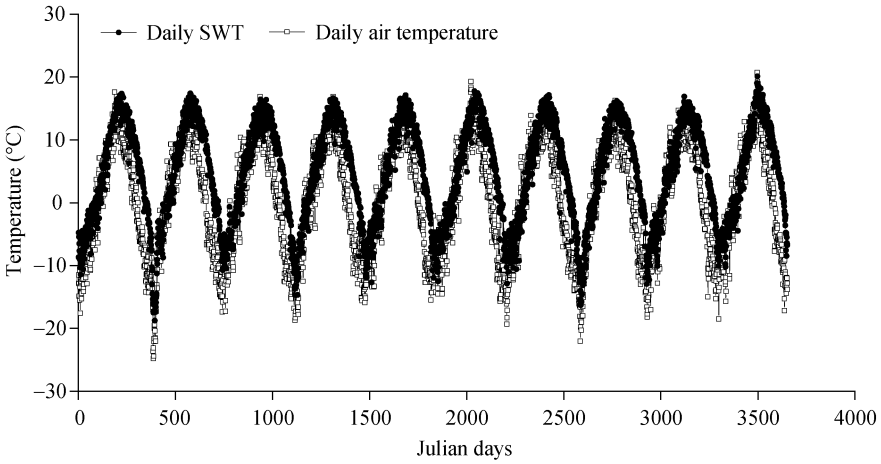

Fig. 3 Daily surface water temperature (SWT) and daily air temperature from 2001 to 2010

perature. Their paths all fluctuated synchronously during a one-year cycle. When the air temperature attained its peaks during cold and warm stages, the SWT values were also in the correspondent positions. During these 10 years, the SWT values ranged from –18.75°C to 20.11°C. Lake SWT at 0°C often indicates the ice cover occurrence in part of the lake. When the SWT continues to descend, the ice cover will expand, and entire surface of the lake will freeze up at last. For simplicity, we used SWT to express the surface temperature for both water or ice cover.

The highest SWT point occurred in 2010, and the lowest point appeared in 2002. The mean value of all highest annual SWT points was 17.30°C, and the mean value of all lowest annual SWT points was –13.30°C. Similarly, the air temperature ranged from –24.80°C to 20.70°C during 2001–2010. The highest temperature also occurred in 2010, and the lowest temperature appeared in 2002. From the daily air temperature and daily SWT records, the daily air temperature was observed to be often lower than the daily SWT during the temperature decreasing phase, whereas they are comparable during the temperature increasing phase.

The annual maximum, annual minimum, and annual mean values of air temperature and SWT from 2001 to 2010 were presented in Fig. 4. The annual maximum values of the air temperature and SWT were almost equal. Nevertheless, relative large differences between air temperature and SWT existed in the annual mean and annual minimum values. The annual mean and annual minimum values of SWT were consistently higher than those of the air temperature, although their fluctuations were similar. The annual mean air temperature fluctuated from 0.22°C to 1.17°C, whereas the variation of the annual mean SWT ranged between 4.18°C and 5.01°C. The average difference between the annual mean air temperature and annual mean SWT was approximately 4.05°C. Similarly, the average difference between the annual minimum air temperature and annual minimum SWT was roughly 5.51°C. However, for the annual maximum values, the difference between air temperature and SWT was only approximately 0.23°C.

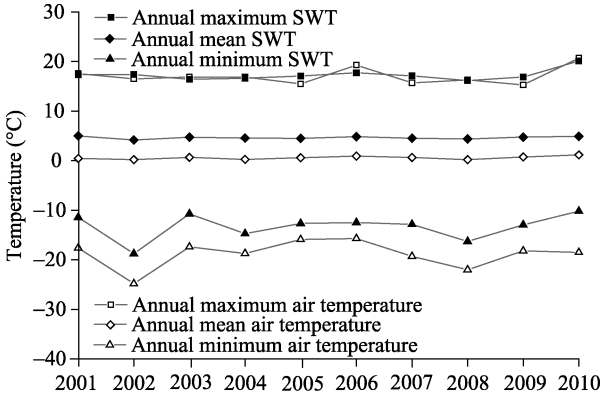

Fig. 4 Annual maximum, annual minimum, and annual mean values for air temperature and surface water temperature (SWT) from 2001 to 2010

Among all the tracks of annual maximum, annual minimum and annual mean values, the annual mean value tracks for air temperature and SWT were the most stable, whereas the annual minimum value tracks for air temperature and SWT were the most undulant (Fig. 4). From 2001 to 2010, the annual minimum air temperature values varied from –24.80°C to –15.70°C, and the annual minimum SWT changed between –18.75°C and –10.19°C. The annual maximum value tracks for air temperature and SWT were stable from 2001 to 2009 and ascended obviously in 2010. Both the annual mean air temperature and annual mean SWT showed slightly increasing trends during the study period. The linear fit slope of the annual mean air temperature was higher than that of the annual mean SWT. The increase rate of the annual mean air temperature was about 0.05°C/a, whereas the increase rate of the annual mean SWT was about 0.01°C/a.

Figure 5 shows the 10-year average daily SWT at about 10:30 a.m. (local solar time) and the average daily air temperature from 2001 to 2010. The daily values were calculated by averaging the temperatures of the same Julian days in these 10 years. Despite the fact that the average daily SWT was generally higher than the average daily air temperature, the 10-year average daily SWT and average daily air temperature changed coincidently. The period from Julian day 20 to 215 described the temperature increasing phase, while the periods from Julian day 0 to 20 and from Julian day 215 to 365 described the temperature decreasing phases.

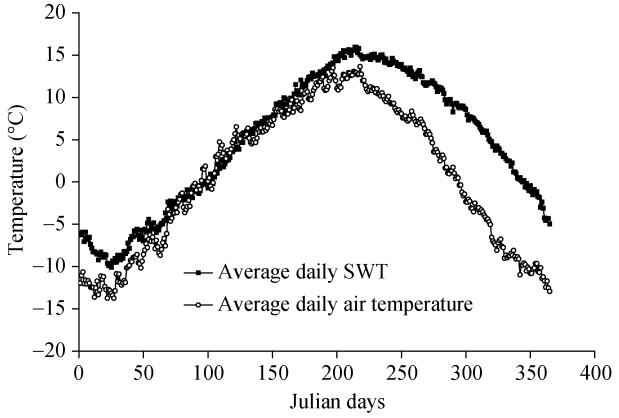

Fig. 5 Ten-year average daily surface water temperature (SWT) and average daily air temperature from 2001 to 2010

Evidently, the differences between the average daily SWT and average daily air temperature during the temperature decreasing phases were relatively larger than those differences during the temperature increasing phase. The average daily temperature difference between air temperature and SWT during the temperature increasing phase was roughly 1.66°C, whereas that in the temperature decreasing phases was about 7.15°C. From Julian day 300 to 340, the difference between the average daily SWT and average daily air temperature exceeded 10°C. The average freeze-up date of Qinghai Lake was approximately at Julian day 345, and the break-up date was approximately at Julian day 100.

Figure 6 shows the 10-year mean values of the monthly average SWT and monthly SWT changes from 2001 to 2010. The period from February to August represented the increasing stage of monthly average SWT, while the period from September to the following January indicated the decreasing stage. The warmest month was August during which the monthly average SWT for the whole lake reached 14.79°C. In August, seven annual maximum values of daily SWT occurred during these 10 years. January was the coldest month of the year, when the monthly average SWT for the whole lake dropped to as low as –8.23°C. According to the statistical data, eight annual minimum values of daily SWT occurred in January during these 10 years. During the period between April and November, the monthly average SWT was over 0°C, while from December to the following March, the monthly average SWT in the lake area was below 0°C. Generally, the monthly SWT trends fluctuated around 0°C. The coldest month (January) and the warmest month (August) all manifested increasing trends from 2001 to 2010 in terms of monthly average SWT. The maximum warming trend also occurred in January, with a rate of approximately 0.16°C/a. In August, the warming rate was roughly 0.07°C/a. The maximum cooling trend occurred in June, with a rate of approximately –0.06°C/a.

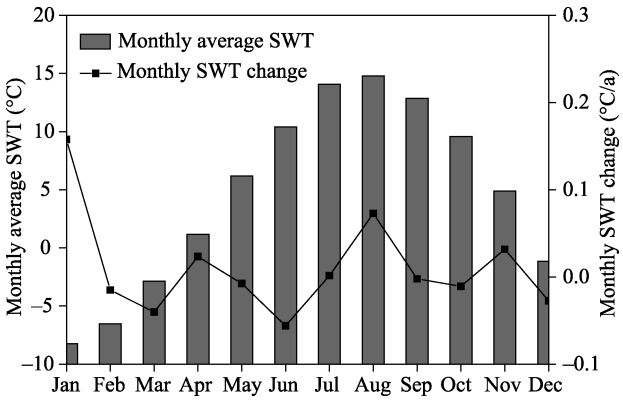

Fig. 6 Ten-year mean values of the monthly average surface water temperature (SWT) and monthly SWT changes from 2001 to 2010

In addition to the retrieval accuracy of SWT, different amounts of available SWT data in different months would cause the differences in calculation accuracy. According to our statistics, the days without any pixel in acceptable quality occurred more frequently from May to September in this study area. Especially in July and August, the total numbers of days with no data reached the maximum because of the enhanced cloud cover. The statistical result about the cloud-contaminated data was in accordance with the observed data of the Gangcha weather station. The total recorded rainy days were also more numerous in the months from May to September, and July and August were also the two months with the maximum number of rainy days all year round. Therefore, there should be less accurate monthly average SWT and monthly SWT changes from May to September than in the other months.

4.3 Spatial changes in SWT

4.3.1 Spatial patterns of the annual average SWT

The spatial patterns of the annual average SWT for

different years were similar to some extent (Figs. 7a–j). The north and the southwest parts of the lake mostly had lower annual average SWTs, and the east and the southeast parts mostly had higher annual average SWTs.

Generally, the spatial pattern of the 10-year mean

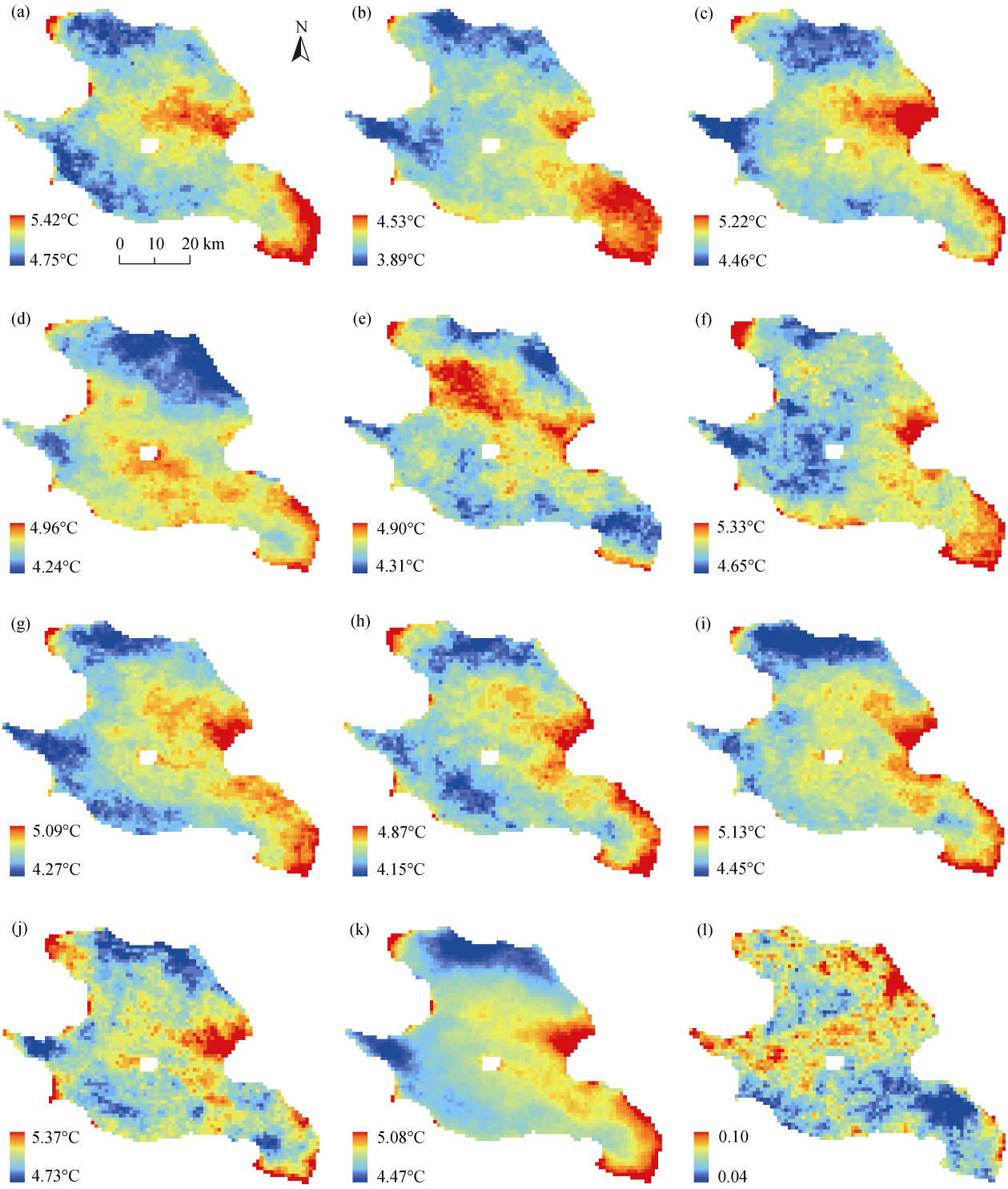

Fig. 7 Spatial patterns of the annual average surface water temperature (SWT). (a)–(j), spatial patterns of the annual average SWT from 2001 to 2010, respectively; (k), spatial pattern of the 10-year mean values of the SWT; (l), spatial variance of the annual average SWT.

SWT was spatially coincident with the annual average SWT, and it also showed obvious spatial heterogeneity (Fig. 7k). The 10-year mean values of SWT changed spatially from 4.47°C to 5.08°C. Locations with the lowest SWT were distributed in the north and southwest shores of the lake, and the SWT became gradually higher from the shores to the central region of the lake. In contrast, the areas with the highest SWT were mainly located at the east and southeast shores of Qinghai Lake, and the SWT became gradually lower from the shores to the central region of the lake.

The spatial variance of the annual average SWT from 2001 to 2010 ranged from 0.04 to 0.10 during these 10 years (Fig. 7l). As a whole, the variance in the north region was a little higher than that in the south region of Qinghai Lake.

The inhomogeneous distribution of the annual average SWT from 2001 to 2010 has a good spatial correspondence with drainage distribution. The shape of the drainage basin and the spatial distributions of the rivers all appeared as asymmetric patterns (Fig. 1). The number of influent rivers was more than 50. However, the rivers were mainly concentrated in the north and northwest sides of the lake, whereas rivers were sparse in the south and southeast sides. Moreover, the river catchment areas in the north and northwest sides of the lake were apparently much bigger than those in the south and southeast sides of the lake. The Buha River in the northwest side of the lake is the biggest river in Qinghai Lake drainage basin, with a drainage area of roughly 14,500 km^2 and an annual runoff of 1.12×10^9 m^3. The rivers in the north side of the lake mainly include Shaliu River, Haergai River, and Quanji River, with annual runoffs of approximately 0.30×10^9, 0.24×10^9, and 0.05×10^9 m^3, respectively (Sun et al., 2007; Li et al., 2010). The runoffs of these four rivers accounted for more than 75% of the total runoff of the Qinghai Lake drainage basin.

The relationship between the spatial patterns of the annual average SWT and the river distribution showed that the rivers in the north and northwest sides of the lake brought cooling effects to the annual average SWT of Qinghai Lake. Furthermore, it seems that the cooling effect of the rivers in the north side of the lake was greater than that in the northwest side, since the low-temperature area was bigger in the north region than in the northwest region of the lake.

Commonly, differences in cooling effects among different rivers would be influenced not only by runoff but also by river water temperature. Since the runoff of the Buha River in the northwest side of the lake was larger than the runoff of the rivers in the north side, it was conjectured that the estuarine temperature of Buha River was relative higher than those of the rivers in the north side of the lake.

The temperature differences among the river estuaries were probably related to the distances between the lake and the mountain watersheds. All the influent rivers of Qinghai Lake take their sources from the mountain areas. According to the investigations at another similar watershed in Northwest China, the water temperature will get warmer with the distance of flow for rivers originated from mountains (Xiayimulati, 2009). The distance between the Qinghai Lake and the mountain watershed of Buha River is 117 km. As for the rivers in the north side of the lake, the distances between the lake and the mountain watershed of these rivers are all shorter than 117 km. Those distances for Shaliu River, Haergai River, and Quanji River are 21 km, 45 km, and 11 km, respectively. Accordingly, the temperature of Buha River in the northwest side of the lake would be relative higher with the increase of flow path length. This was probably the reason for the occurrence of spatial difference in the cooling effect in Qinghai Lake.

4.3.2 Annual cyclical changes of the SWT spatial patterns

Similar to the seasonal cycles of air temperature, the annual cyclical changes of the SWT spatial patterns also varied seasonally (Fig. 8). Generally, the spatial changes of SWT show a seasonal inversion pattern. The relative positions between the high-temperature and low-temperature areas from January to June were, to some extent, opposite to those from July to December. In January, the temperature was distinctly lower in the northeast area than in the southwest area. Then, the low-temperature areas moved to the north region of the lake, and the high-temperature areas moved to the south and east regions in February.

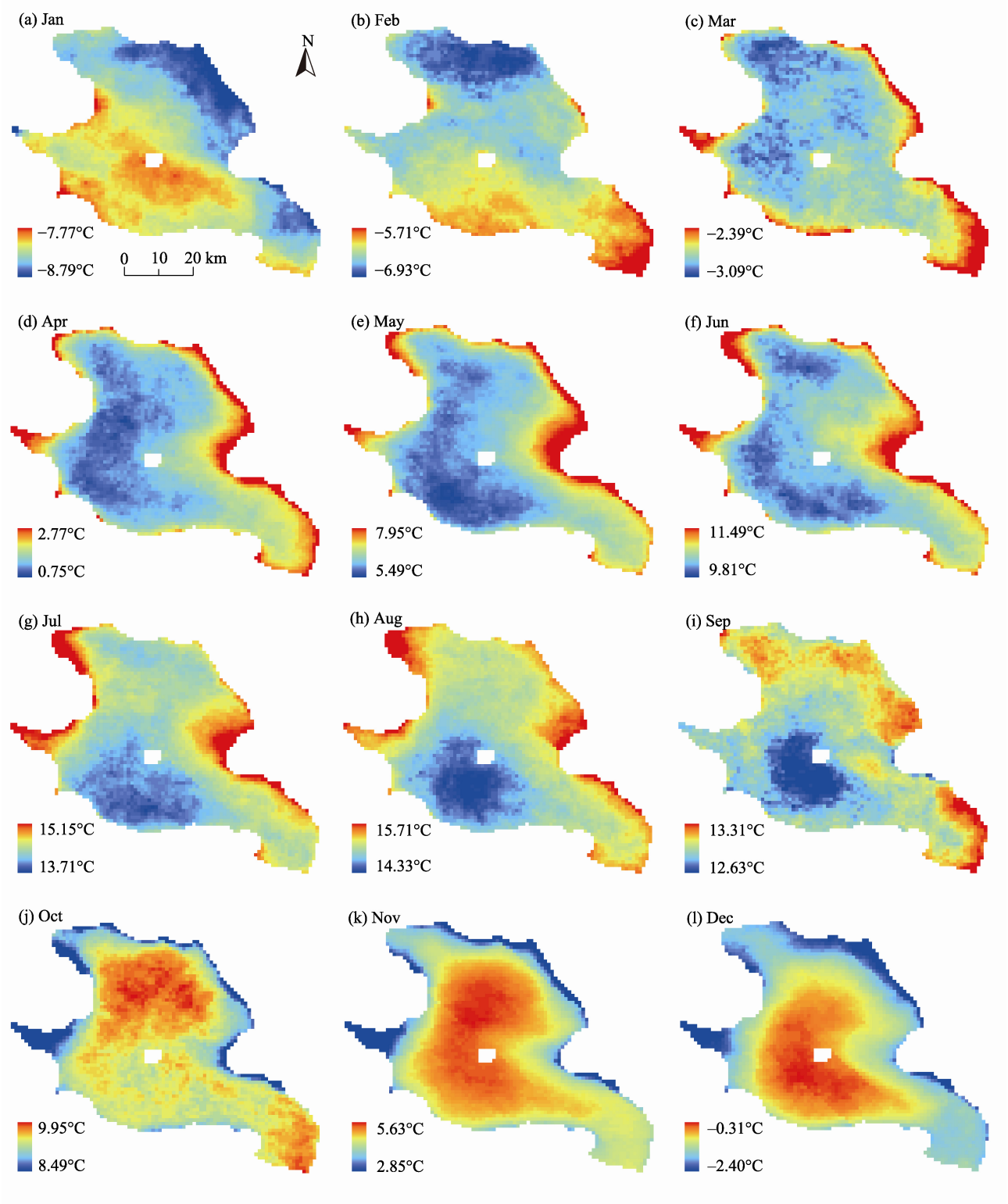

Fig. 8 Annual cyclical changes of the surface water temperature (SWT) spatial patterns from January to December

From March to April, the low-temperature areas moved gradually to the south and the central regions of the lake. Correspondingly, the shore areas of the lake had relatively higher temperature during this time. The SWT spatial patterns were similar from April to June. The central and the south regions of the lake had

relatively lower temperature during this period. In July, the low-temperature areas were concentrated in the southwest region of the lake, and the high-temperature areas were mainly located in the north and the northeast regions of Qinghai Lake.

From July to September, the center of the low-temperature area moved slowly to the center of the lake. In October, the previous low-temperature area in the central region of the lake disappeared, and the area in the north shore became a new low-temperature region. The center of the high-temperature area was located in the north region of the lake during this month. Afterwards, the high-temperature area spread to the center of Qinghai Lake in November. Then, the center of the high-temperature area moved gradually to the south direction from November to December.

With regard to the lakeshore, the monthly SWT changes also showed distinctive periodical phenomena (Fig. 8). In January and February, the north shore showed lower SWTs, whereas the south shore had higher SWTs. Then, from March to September, the average monthly SWTs were higher in most of the lakeshore than in the center of the lake. Afterwards, the average monthly SWTs were lower in most of the lakeshore than in the center of the lake from October to December.

Generally, the north areas of the lake had higher amplitudes of variation in average monthly SWT values during the seasonal cycle. During the temperature increasing period from February to August, the low-temperature area in the north region of the lake changed to a high-temperature area, whereas the high-temperature area in the south region of the lake transformed into a low-temperature area. During the temperature decreasing period from September to the following January, the low- and high-temperature areas showed a different reversion pattern. Accordingly, compared with the condition in the south area, the temperature in the north area of the lake changed more easily following changes in air temperature.

Many studies have shown statistically significant correlation between lake depth and heat budgets (Gorham, 1964). Under given climatic and meteorological factors, lake depth is one of the dominant factors that control SWT variation amplitude (Balsamo et al., 2010). For Qinghai Lake, the water depths are smaller at the shore areas than in the center of the lake (Fig. 9). In particular, in the area near the north shore, the slope of the lake basin topography is gentle, and the water is relatively shallow with a depth blew 20 m (Shen and Kuang, 2003). Thus, the average monthly SWT of the shore areas especially the north shore areas warmed up faster during the temperature increasing period, whereas it cooled down faster during the temperature decreasing period in the seasonal cycle.

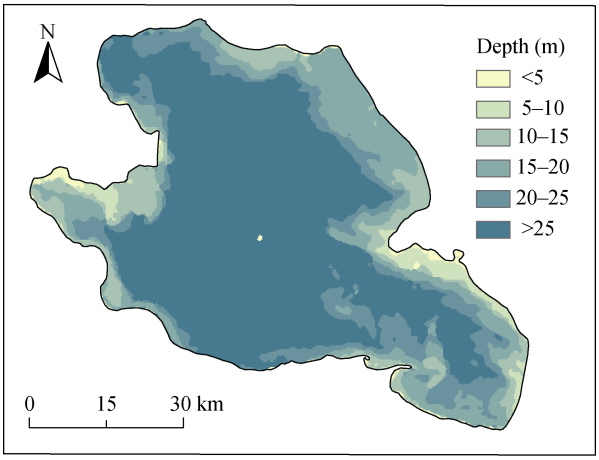

Fig. 9 Bathymetry map of Qinghai Lake (cited from Shen and Kuang, 2003)

By contrast, the water depths of the central areas and some south-central shore areas of the lake are generally more than 25 m. Corresponding with the bathymetry features of the central areas and the south-central shore areas, the amplitudes of SWT variation were lower in these areas than in the other shore areas and the north part of the lake. Moreover, in Qinghai Lake, the changes in SWT spatial patterns were considered as a possible indicator of the spatial difference in the water-heating capacity. According to the hydrological data (Sun et al., 2007; Liu et al., 2009), the fresh water flows into Qinghai Lake primarily comes from rivers in the northwest and north sides of the lake. Therefore, the heat capacities of water are possibly lower near the north and northwest areas due to lower salinity. Synthetically, due to the effects of the lake basin topography and the water salinity difference, the variation amplitudes of average monthly SWTs in the north and the shore areas were

relatively greater than those in the central area.

5 Conclusions

In this paper, the spatial-temporal variations of SWTs in Qinghai Lake from 2001 to 2010 were analyzed using the time series of water surface temperature recorded in MODIS products. Overall, the daily SWT during the satellite passing time was higher than the daily air temperature. The annual maximum values of air temperature and SWT were almost the same. However, relatively larger differences between air temperature and SWT existed in the annual mean and annual minimum values. The tracks of the annual minimum values of both air temperature and SWT were more undulant than those of the annual minimum and annual mean values.

From the 10-year average daily SWT and average daily air temperature, we judged that the period from Julian day 20 to 215 showed a temperature increasing phase. The differences between average daily SWT and average daily air temperature during the temperature decreasing phases were relatively larger than those during the temperature increasing phase. The annual average air temperature and the annual average SWT all showed increasing trends from 2001 to 2010. The increasing rate of the annual average air temperature was approximately 0.05°C/a, and the increasing rate of the annual average SWT was about 0.01°C/a.

The spatial patterns of annual average SWT in different years were similar to some extent. The north and southwest parts of the lake mostly had lower annual average SWTs, and the east and southeast parts mostly had higher annual average SWTs. The inhomogeneous distribution of the annual average SWT from 2001 to 2010 showed a good spatial correspondence with the drainage distribution.

The SWT spatial changes showed a seasonal reversion pattern. From January to December, the relative positions of the high-temperature areas changed stepwise from the south to the north regions and then back to the south region, whereas the low-temperature areas showed an adverse annual cyclical trace. The north area of the lake had higher average monthly SWT amplitudes during the seasonal cycle. The spatial patterns of SWT variation amplitude were shaped mainly by the topography of the lake basin, and water salinity difference possibly contributed to these effects.

Acknowledgments

The study was supported by the National Basic Research Program of China (2012CB417001) and the National Natural Science Foundation of China (41271125).

References

Alcântara E H, Stech J L, Lorenzzetti J A, et al. 2010. Remote sensing of water surface temperature and heat flux over a tropical hydroelectric reservoir. Remote Sensing of Environment, 114(11): 2651–2665.

Arnell N, Bates B, Lang H, et al. 1996. Hydrology and freshwater ecology. In: Watson R T, Zinyowera M C, Moss R H, et al. Climate Change 1995: Impacts, Adaptations, and Mitigation of Climate Change—Scientific-Technical Analysis, Contribution of Working Group II to the Second Assessment Report of the Intergovernmental Panel on Climate Change. Cambridge: Cambridge University Press, 325–364.

Balsamo G, Dutra E, Stepanenko V M, et al. 2010. Deriving an effective lake depth from satellite lake surface temperature data: a feasibility study with MODIS data. Boreal Environment Research, 15(2): 178–190.

Barton I J, Prata A J. 1995. Satellite derived sea surface temperature data sets for climate applications. Advances in Space Research, 16(10): 127–136.

Becker M W, Daw A. 2005. Influence of lake morphology and clarity on water surface temperature as measured by EOS ASTER. Remote Sensing of Environment, 99(3): 288–294.

Bussières N, Schertzer W M. 2004. The evolution of AVHRR-derived water temperatures over lakes in the Mackenzie Basin and hydrometeorological applications. Journal of Hydrometeorology, 4: 660–672.

Chavula G, Brezonik P, Thenkabail P, et al. 2009. Estimating the surface temperature of Lake Malawi using AVHRR and MODIS satellite imagery. Physics and Chemistry of the Earth, 34(13–16): 749–754.

Cho H Y, Lee K H. 2012. Development of an air-water temperature relationship model to predict climate-induced future water. Journal of Environmental Engineering, 138(5): 570–577.

Crosman E T, Horel J D. 2009. MODIS-derived surface temperature of the Great Salt Lake. Remote Sensing of Environment, 113(1): 73–81.

Ekercin S, Örmeci C. 2010. Evaluating climate change effects on water and salt resources in Salt Lake, Turkey using multitemporal SPOT imagery. Environmental Monitoring and Assessment, 163(1–4): 361–368.

Emery W J, Yu Y. 1997. Satellite sea surface temperature patterns. International Journal of Remote Sensing, 18(2): 323–334.

Fily M, Royer A, Goïta K, et al. 2003. A simple retrieval method for land surface temperature and fraction of water surface determination from satellite microwave brightness temperatures in sub-arctic areas. Remote Sensing of Environment, 85(3): 328–338.

Gorham E. 1964. Morphometric control of annual heat budgets in temperate lakes. Limnology and Limnology and Oceanography, 9(4): 525–529.

Handcock R N, Gillespie A R, Cherkauer K A, et al. 2006. Accuracy and uncertainty of thermal-infrared remote sensing of stream temperatures at multiple spatial scales. Remote Sensing of Environment, 100(4): 427–440.

Hook S J, Vaughan R G, Tonooka H, et al. 2007. Absolute radiometric in-flight validation of mid infrared and thermal infrared data from ASTER and MODIS on the Terra Spacecraft using the Lake Tahoe, CA/NV, USA, automated validation site. IEEE Transactions on Geoscience and Remote Sensing, 45(6): 1798–1807.

Kothandaraman V, Evans R L. 1972. Use of Air-Water Relationships for Predicting Water Temperature. Illinois State Water Survey, Urbana, Report of Investigation 69. Urbana, USA: Authority of the State of Illinois-Ch, 1–14.

Li H W, Beschta R L, Kauffman J B, et al. 2000. Geomorphic, hydrologic and ecological connectivity in Columbia River watersheds: implications for endangered salmonids. In: Completion Report to the Environmental Protection Agency Star Program, R82-4774-010. Oregon State University, USA.

Li Y T, Li X Y, Cui B L, et al. 2010. Trend of streamflow in Lake Qinghai basin during the past 50 years (1956–2007). Journal of Lake Sciences, 22(5): 757–766.

Liu J, Wang F, Yu F L. 2009. Variation tendency prediction of dynamic water level in Qinghai Lake. Journal of Hydraulic Engineering, 40(3): 319–327.

Livingstone D M. 2003. Impact on secular climate change on the thermal structure of a large temperate central European lake. Climatic Change, 57(1–2): 205–225.

Oesch D C, Jaquet J M, Hauser A, et al. 2005. Lake surface water temperature retrieval using advanced very high resolution radiometer and Moderate Resolution Imaging Spectroradiometer data: validation and feasibility study. Journal of Geophysical Research, 110, doi: 10.1029/2004JC002857.

Parkinson C L. 2003. Aqua: an earth-observing satellite mission to examine water and other climate variables. IEEE Transactions on Geoscience and Remote Sensing, 41(2): 173–183.

Plattner S, Mason D M, Leshkevich G A, et al. 2006. Classifying and forecasting coastal upwellings in Lake Michigan using satellite derived temperature images and buoy data. Journal of Great Lakes Research, 32(1): 63–76.

Rani N, Sinha P K, Prasad K, et al. 2011. Assessment of temporal variation in water quality of some important rivers in middle Gangetic plains, India. Environmental Monitoring and Assessment, 174(1–4): 401–415.

Reinart A, Reinhold M. 2008. Mapping surface temperature in large lakes with MODIS data. Remote Sensing of Environment, 112(2): 603–611.

Schneider P, Hook S J, Radocinski R G, et al. 2009. Satellite observations indicate rapid warming trend for lakes in California and Nevada. Geophysical Research Letters, 36, doi: 10.1029/2009GL040846.

Sha W Y, Shao X M, Huang M. 2002. Climate warming and its impact on natural regional boundaries in China in the 1980s. Science in China: Earth Sciences, 32(4): 317–326.

Shen F, Kuang D B. 2003. Remote sensing investigation and survey of Qinghai Lake in the past 25 years. Journal of Lake Sciences, 15(4): 289–296.

Sun Y L, Li X Y, Xu H Y. 2007. Daily precipitation and temperature variations in Qinghai Lake watershed in recent 40 years. Arid Meteorology, 25(1): 7–13.

Torgersen C E, Faux R N, McIntosh B A, et al. 2001. Airborne thermal remote sensing for water temperature assessment in rivers and streams. Remote Sensing of Environment, 76(3): 386–398.

Trumpickas J, Shuter B J, Minns C K. 2009. Forecasting impacts of climate change on Great Lakes surface water temperature. Journal of Great Lakes Research, 35(3): 454–463.

Wan Z, Dozier J. 1996. A generalized split-window algorithm for retrieving land-surface temperature from space. IEEE Transactions on Geoscience and Remote Sensing, 34(4): 892–905.

Wan Z. 1999. MODIS Land-Surface Temperature Algorithm Theoretical Basis Document (LST ATBD): Version 3.3. Institute for Computational Earth System Science, University of California, Santa Barbara.

Wan Z, Zhang Y, Zhang Q, et al. 2004. Quality assessment and validation of the MODIS global land surface temperature. International Journal of Remote Sensing, 25(1): 261–274.

Wan Z M, Zhang Y L, Zhang Q C, et al. 2002. Validation of the land-surface temperature products retrieved from Terra Moderate Resolution Imaging Spectroradiometer data. Remote Sensing of Environment, 83(1–2): 163–180.

Wang J H, Tian J H, Li X Y, et al. 2011. Evaluation of concordance between environment and economy in Qinghai Lake Watershed, Qinghai-Tibet Plateau. Journal of Geographical Sciences, 21(5): 949–960.

Wang W H, Liang S L, Meyers T. 2008. Validating MODIS land surface temperature products using long-term nighttime ground measurements. Remote Sensing of Environment, 112(3): 623–635.

Wloczyk C, Richter R, Borg E, et al. 2006. Sea and lake surface temperature retrieval from Landsat thermal data in Northern Germany. International Journal of Remote Sensing, 27(12): 2489–2502.

Wooster M, Patterson G, Loftie R, et al. 2001. Derivation and validation of the seasonal thermal structure of Lake Malawi using multi-satellite AVHRR observations. International Journal of Remote Sensing, 22(15): 2953–2972.

Wu S H, Yin Y H, Zheng D, et al. 2005. Climate changes in the Tibetan Plateau during the last three decades. Acta Geographica Sinica, 60(1): 3–11.

Xiayimulati. 2009. Characteristics of water temperature change of inland rivers in western part of Tianshan Mountains in last 50 years. Journal of China Hydrology, 29(2): 84–86.

Zhao L, Ping C L, Yang D Q, et al. 2004. Changes of climate and seasonally frozen ground over the past years in Qinghai-Xizang (Tibetan) Plateau, China. Global and Planetary Change, 43(1–2): 19–31.

Zheng D, Lin Z Y, Zhang X Q. 2002. Progress in studies of Tibetan Plateau and global environmental change. Earth Science Frontiers, 9(1): 95–102.

Zhu S J, Chang Z F. 2011. Temperature and precipitation trends in Minqin Desert during the period of 1961–2007. Journal of Arid Land, 3(3): 214–219.